Theoretical study to evaluation of corrosion inhibition performance of two thiocarbohydrazide inhibitors

Sayyed Mostafa Habibi-Khorassani[a], Maryam Dehdab[b,*], Mahdieh Darijani[a]

[a]Department of Chemistry, University of Sistan and Baluchestan, P.O. BOX 98135-674, Zahedan, Iran

[b]Young Researchers and Elite Club, Bushehr Branch, Islamic Azad University, Bushehr, Iran

Abstract

Molecular dynamics (MD) simulation and Density functional theory (DFT) methods were applied to the two thiocarbohydrazides derivatives (T1 and T2) as corrosion inhibitors in aqueous phase. Experimental results has shown that the corrosion rate follows the order: T1>T2. Quantum chemical parameters such as hardness (η), electrophilicity (ω), polarizability (α), dipole moment (μ) , E_{HOMO} (the energy of the highest occupied molecular orbital), E_{LUMO} (the energy of the lowest unoccupied molecular orbital), Electronegativity (χ), the total amount of electronic charge transferred (ΔN), Lipophilicity, total negative charges on the whole of the molecule (TNC), molecular volume (MV), surface area and Fukui index have been calculated. The results of quantum chemical confirm that T2 is a better inhibitor than T1. Molecular dynamics simulation results showed that T2 inhibitor has the higher negative interaction energy as compared to the T1 inhibitor. Results of DFT and MD simulations calculations confirm that T2 has more inhibition efficiency than T1, which is in good agreement with the experimentally inhibition efficiency data reported.

Keywords: Corrosion inhibitor; quantum chemical; molecular dynamic simulation; carbon steel.

Introduction

Corrosion is more than just an inevitable natural phenomenon; Corrosion can be very expensive as well as unsafe; it is very important from the points of view of economics. Acid solutions are used extensively in industry such as acid pickling, industrial acid cleaning, acid descaling, and oil well acidizing. The sample is immersed in an acid pickling bath to remove undesirable scale. After the removal of the scale, the acid might attack the metal.

Mild steel is an important structural material in many industries equipment due to its low cost and excellent mechanical properties. Among the various methods that prevent or decrease the corrosion rates in an acidic medium, the use of corrosion inhibitors is best known and most useful methods in the industry. The corrosion rate of metals may be reduced by the addition of inorganic or organic compounds, called inhibitors, to their environment.

*Corresponding author: Maryam Dehdab
Tel: +98 (77) 33682307, Fax: +98 (77) 33682307
E-mail: dehdab37@gmail.com

Numerous experimental works have been devoted to corrosion inhibition, whereas theoretical studies (molecular dynamic simulation and Quantum chemical calculation) appeared only recently. A detailed understanding of the chemical interaction between the inhibitor and the substrate is the key to understanding and control of corrosion inhibition.

However, a strong weakness of the Quantum chemical approach is the often used to study the simple systems and calculation of electronic interactions is huge and time-consuming. Molecular dynamics (MD) simulation has been effective tool often used to the inhibitor –surface interaction description [1-4] successful research has been performed in the scope of corrosion inhibition using different computational approaches [5-18].

The purpose of this paper is to compare theoretical results of Corrosion inhibition of two thiocarbohydrazides derivatives ((*N,N'*-[2,2'-thiocarbonyl bis(hydrazine-2,1-diyl) bis (thioxomethylene)] dibenzamide (T1) and *N,N'*-[2,2'-thiocarbonylbis(hydrazine-2,1- diyl) bis (thioxomethylene)] bis (4-methoxybenzamide) (T2))with

experimental data recently reported as good corrosion inhibitors on carbon steel in acidic solution [19]. Experimental data shows that the corrosion rate follows the order: T2> T1, which indicates that T2 exhibits the better inhibition performance among the studied two inhibitors. Herein, in this study, inhibition effects of two thiocarbohydrazide derivatives (Figure 1) have been studied on corrosion of carbon steel using a number of The global reactivity descriptors such as hardness (η), electrophilicity ($\boldsymbol{\omega}$), polarizability ($\boldsymbol{\alpha}$), dipole moment ($\boldsymbol{\mu}$) and another quantum chemical parameters such as E_{HOMO} (the energy of the highest occupied molecular orbital), E_{LUMO} (the energy of the lowest unoccupied molecular orbital), Electronegativity ($\boldsymbol{\chi}$), the total amount of electronic charge transferred (ΔN), Lipophilicity, total negative charges on the whole of the molecule (TNC), molecular volume (MV), surface area and Fukui index. In order to obtain the adsorption energies of two thiocarbohydrazide derivatives upon the Fe (110) surface Molecular dynamics (MD) simulation was performed.
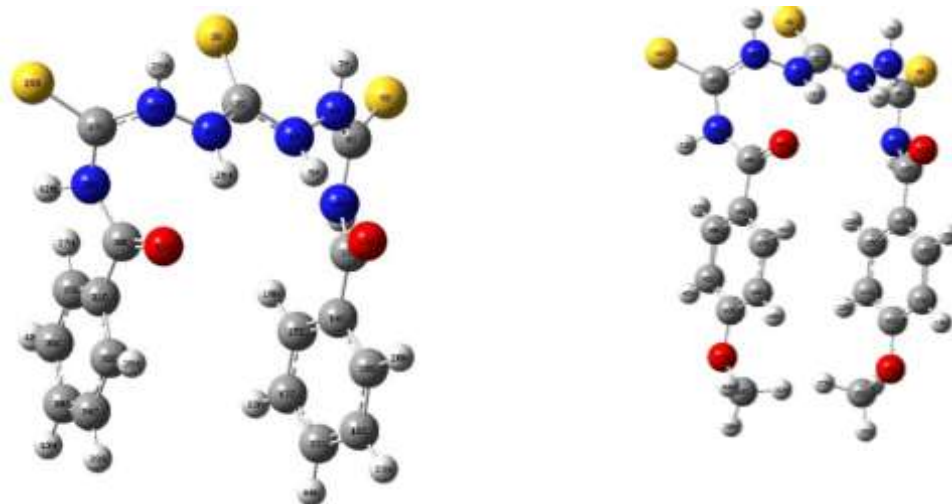

Figure 1. The optimized structures of the studied two thiocarbohydrazides derivatives

Computational details

Quantum chemical calculations

Quantum chemical calculations were performed for two thiocarbohydrazide derivatives as corrosion inhibitors using the DFT/B3LYP method with basis set of 6-311++G** basis set [20-22] by the Gaussian 03 program [23]. The two structures reported were fully optimized and their number of imaginary frequencies (NIMAG) was zero, thereby confirming their existence at positions of minima (global or local) on the potential energy surface (PES). Generally, the phenomenon of electrochemical corrosion occurs in the aqueous phase, and it is expected that inhibiting molecules in solution behave differently from those in a vacuum, so it is necessary to consider the effect of solvent in the calculations. Hence, the effect of solvent in the calculations was considered with Tomasi's polarized continuum model [24].

The global reactivity descriptors determine the chemical behavior of a molecular species by considering it as a whole, as defined within the density functional theory of Parr, Pearson and Yang [25,26].

Applying the finite difference approximations, for an *N*-electron system having total energy *E*, Global hardness ($\boldsymbol{\eta}$) and Electronegativity χ can be expressed as

$$\boldsymbol{\eta} = \frac{1}{2} \left[\frac{\partial^2 E}{\partial N^2} \right]_{v(r)} = \frac{I-A}{2} \qquad (1)$$

$$\boldsymbol{\mu} = -\chi = \left[\frac{\partial E}{\partial N} \right]_{v(r)} = \frac{I+A}{2} \qquad (2)$$

Where $(\boldsymbol{r})$, $\boldsymbol{\mu}$, *I* and *A* are external potentials, chemical potentials, the ionization potential and electron affinity, respectively. Applying the Koopmans' theorem, the ionization potential and electron affinity of a molecule can be expressed in terms of the energies of the frontier molecular

orbitals (FMOs) thus χ and η can be expressed as[27, 28].

$$\boldsymbol{\eta} = \frac{1}{2} (E_L - E_H) \qquad (3)$$

$$\chi = -\frac{1}{2} (E_L + E_H) \qquad (4)$$

Where $\boldsymbol{E_H}$ and $\boldsymbol{E_L}$ associated with the frontier molecular orbital HOMO and LUMO, respectively.

Global electrophilicity index ($\boldsymbol{\omega}$), has been proposed by Parr et al is the measure of the electrophilic tendency of a molecule [29]; it is can be obtained from the definitions of global hardness and the electronegativity as follows:

$$\boldsymbol{\omega} = \frac{\chi^2}{2\eta} \qquad (5)$$

This was proposed as a measure of the electrophilic power of a molecule. A good nucleophile is characterized by low value of $\boldsymbol{\omega}$; while a good electrophile is characterized by high value $\boldsymbol{\omega}$ [30].

The higher value of $\boldsymbol{\omega}$, the higher capacity of the molecule to accept electrons.

The total amount of electronic charge transferred, Δ*N*, from the inhibitor to metallic surface calculated according to Pearson theory through the equation (6):

$$\Delta N = \frac{\chi_{Fe} - \chi_i}{2(\eta_{Fe} + \eta_i)} = \frac{\varphi_{Fe} - \chi_i}{2(\eta_{Fe} + \eta_i)} \qquad (6)$$

The theoretical values of $\boldsymbol{\chi_{Fe}}$ and η_{Fe} were employed 7 eVmol^{-1} and 0 eVmol^{-1} for bulk iron, respectively by assuming that for a bulk metallic *I = A*, because they are softer than the neutral metallic atoms [31,32]. If $\boldsymbol{\Delta N > 0}$ iron is acceptor and inhibitor is donor and $\boldsymbol{\Delta N < 0}$, the case is reverse.

Actually, the value of 7.0 eV corresponds to the free electron gas Fermi energy of iron in the free electron gas model. Where the electron–electron interaction is neglected, and the use of this value as $\boldsymbol{\chi_m}$is conceptually wrong [33,34]. Therefore, some researchers demonstrated that the work function

($\boldsymbol{\varphi_m}$) of a metal surface is an appropriate measure of its electronegativity and should be used in the estimation of $\boldsymbol{\Delta N}$ [35, 36] .

In this study we had chosen Fe (1 1 0) surface among other optional Fe surfaces, where the $\boldsymbol{\varphi_m}$ value obtained from DFT calculations is 4.82 eV for Fe (110) surfaces [37].

The electric dipole polarizability ($\boldsymbol{\alpha}$), is a measurement of the linear response of the electron density in the presence of an infinitesimal electric field F and it descript a second order variation in energy:

$$\boldsymbol{\alpha} = -\left(\frac{\partial^2 E}{\partial^2 F_a \partial^2 F_b}\right) \qquad a,b = x, y, z \ (7)$$

The mean polarizability ($\boldsymbol{\alpha}$) is calculated through the equation (8):

$$\boldsymbol{\alpha} = \frac{1}{3}\left(\boldsymbol{\alpha_{xx}} + \boldsymbol{\alpha_{yy}} + \boldsymbol{\alpha_{zz}}\right) \qquad (8)$$

It was discovered that polarizabilities are inversely proportional to the third power of the hardness values [38, 39]. On the basis of this fact, with increasing softness, a molecule becomes more polarizable.

The local reactivity has been analyzed by means of Fukui functions(($\boldsymbol{F^+}$(for atom k as an electrophile) $\boldsymbol{F^-}$(for atom k as a nucleophile)), which are an indication of the reactive centers within the molecules. With respect to a finite difference approximation, the condensed Fukui functions were calculated as an atom k in a molecule with N electrons [33]:

$$\boldsymbol{F^+(r) = q_k(N + 1) - q_k(N)}$$
(9)
$$\boldsymbol{F^-(r) = q_k(N) - q_k(N - 1)}$$
(10)

Where $q_k(N)$, $q_k(N+1)$, and $q_k(N-1)$ are the charges of the k_{th} atom for N, N + 1, and N - 1 electron systems, respectively.

Molecular dynamics simulation

Molecular dynamics simulation (MD simulation) is popular to studies the interaction between an inhibitor and metal surface. The adsorption process of two thiocarbohydrazide derivatives on iron surface (Fe(110)) is simulated by using the Forcite molecular dynamics module the Materials Studio 6.0 program developed by Accelrys Inc [40]. As earlier observed for Fe [41], the most stable plane would be Fe(110). Herein, in this study we had chosen Fe(110) surface among other optional Fe surfaces for simulation. The Fe crystal was cleaved along the (110) plane.

The interaction between Fe (110) surface and inhibitor molecules is carried out in a simulation box (37.23×37.23×72.11 Å) with periodic boundary conditions. A vacuums lab of 50Å height is kept over the Fe(110) surface. Coulomb and van der Waals interactions were calculated by using the Ewald method. During the simulation process all the atoms in the Fe (110) surface were kept frozen and inhibitors are allowed to interact with the metal surface freely. The interaction of inhibitors on the Fe(110) surface is then simulated by pcff(The polymer consistent force field) force field. The single inhibitor along with 400 water molecules, 5Cl$^-$ ions, 5 H_3O^+ ions were used for the simulations in each case. The use of the water molecules, Cl$^-$ ions and H_3O^+ ions is important because electrochemical corrosion inhibition process occurs in aqueous solution and acidic media. The simulation was performed at 298 K, canonical ensemble (NVT), with a time step of 1.0fs and a simulation time of 50 ps. the geometry of the system was optimized. Then, the dynamic process was carried out until the entire system reached equilibrium, at which both the

temperature and the energy of the system were balanced.

The interaction energy between the metal and the inhibitors was then considered as [40];

$$E_{int} = E_{(Fe.-X)} - (E_X + E_{Solution} + E_{Fe})$$ (11)

Where $E_{(Fe.-X)}$ is the total energy of the full system (the surface with the water molecules, ions and adsorbed inhibitor molecule), E_X is the energy of the inhibitor without the surface, the water molecules and ions, $E_{Solution}$ is the energy of only the water molecules and ions and E_{Fe} is the energy of Fe(110) surface without the inhibitor , the water molecules and ions.

Results and discussion

Quantum chemical methods are ideal tools for investigating reactivity parameters of the inhibitors and are able to provide an insight into the inhibitor–surface interaction.

The frontier orbitals of chemical species are very important in defining their reactivity. The global molecular reactivity was investigated *via* analysis of the frontier molecular orbitals (FMO) in terms of interaction between the frontier orbitals, involving the HOMO and the LUMO [42]. According to frontier orbital theory, the interaction of inhibitors mainly occurred on the highest occupied molecular orbital (HOMO) and lowest unoccupied molecular orbital (LUMO).

Inhibitors that can donate electrons to unoccupied *d* orbitals of metal surfaces and can also accept free electrons from the metal surface are good candidates for corrosion inhibitors.

E_{HOMO} describes the electron donating ability of the molecule. Therefore, the higher the HOMO energy of the inhibitor, the greater the trend of offering electrons to an appropriate acceptor with a low empty molecular orbital energy. On the other hand, the energy of LUMO, denotes the ability of the molecule to accept electrons using π^* orbitals to form π - back bonds. The lower value of E_{LUMO}, the easier the acceptance of electrons from metal surface. The inhibition efficiency increases with increasing HOMO energy level and decreasing LUMO energy level [43].

Table 1 present the calculated values of E_{HOMO} and E_{LUMO} for the studied two inhibitors. It is clear that E_{HOMO} in case of T2 is higher than T1 which enhance the assumption that T2 will adsorb more strongly on iron surface than T1. From Table 1, it can be concluded that the trend obtained for E_{LUMO}, that the capability of accepting electrons obey the order: T1 > T2. This is not compatible well with the result (inhibition efficiencies) obtained from the experiments.

Table 1. Theoretic quantities calculated at B3LYP/6311++G** level for the studied two thiocarbohydrazides derivatives in aqueous phase

	E_{HOMO} (ev)	E_{LUMO} (ev)	η (ev)	χ (ev)	ω (ev)	ΔN (e)	α (a.u.)	MV (cm³/mol)	surface area(cm²/mol)	log$P$	μ (Debye)
T2	-6.52	-2.30	2.11	4.41	4.62	1.20	551.47	213.1	705.41	3.74	18.62
T1	-6.57	-2.41	2.08	4.49	4.85	1.22	484.59	105.6	620.47	4.24	14.42

Global hardness (η) measures the resistance of an atom to a charge transfer [25]; So, harder inhibitors tend to show lower reactivity and greater stability, unlike the softer ones that readily undergo changes in electron density during interaction with metals.

Pearson expressed the hard and soft acid and base (HSAB) principle[44,45] . Corrosion inhibitors can be viewed from the HSAB principle and described as hard, soft, or borderline inhibitors.

In accordance with the HSAB principle, hard acids form complexes with hard bases and soft acids form complexes with soft bases. Borderline acids form complexes with either soft or hard bases. In the research of corrosion inhibition chemistry, bulk iron is considered as soft acid, this would imply that the softest bases inhibitors are most effective for corrosion of these metals. As indicated in Table 1, the values of Global hardness are not in accordance to the experimentally determined inhibition efficiency.

Electronegativity χ [46] can be expressed with the equation (4) and Electronegativity values studied inhibitors are listed in Table 1. From Table 1, we can see that, among thiocarbohydrazide derivatives, T2 compound show lower χ, this effect increases donating electron to the metallic surface which may be attributed to electron donor group (methoxy). As a result, electron flow from T2 compound is potentially more favorable than T1, resulting in higher inhibition efficiency.

The term electrophilicity (ω) measures the electron-attracting power of chemical species for a molecular system. According to the definition, this index plays a fundamental role in determining the flow of electrons between metal surface and inhibitors. An inhibitor with a high ω value will naturally be more disposed to accepting electrons. A good electrophile is characterized by a high value of ω and contrariwise a good nucleophile is characterized by lower value of ω. For this reason, a molecule that have large nucleophilicity value is a good corrosion inhibitor while a molecule that have large electrophilicity value is ineffective against corrosion. In our present study, T2 is the stronger nucleophile than T1.

Using the work function, φ_{Fe} value of 4.82 eV for Fe (110) surfaces and global hardness, η_{Fe} value of 0 eV/mol for iron atom, the fraction of electrons transferred from thiocarbohydrazide derivatives to the iron surface, was calculated.

According to Lukovits᾽ s study [47], if $\Delta N < 3.6$, the inhibition efficiency increased by increasing the electron donor property of inhibitor. The obtained values of ΔN tabulated in Table 1 are all below 3.6 and the results show that the electron donor substitution in T2 lead to increase in ΔN value. In this study, the fraction of electrons transferred of two thiocarbohydrazide derivatives are positive then the studied inhibitors were the donor of electrons, and the carbon steel surface was the acceptor.

T2 is found to have the Maximum E_{HOMO} and ΔN values, these results support the assertion that it had the greatest ability of offering electrons and the highest inhibition efficiency.

Another parameter which is used in the corrosion inhibition studies is Dipole moment. Dipole moment is the measure of net polarity in a molecule. According to some literatures, with increasing Dipole moment, inhibition effectiveness becomes higher[48], yet others have proposed the opposite

correlation, that is, The low value of dipole moment probably decreases the adsorption on the metal surface, the dipole moment values for two the studied inhibitors are listed in Table 1.

In the current work, the results support former viewpoint, T2 has a higher value (18.62 Debye) of the dipole moment than T1 (14.41 Debye).

Molecular volume (MV) and surface area values of the molecules illustrates possible metal surface coverage by the inhibitor. Large MV and surface area values for inhibitors can be attributed to more coverage of the metal surface. The corrosion rate decreases as the volume and surface area of the molecules increases due to the enhancement of large protection the metal surface. A comparison of the MV and surface area values support that the trend in the MV and surface area values are compatible well with the experimentally determined inhibition efficiencies.

Polarizability is the ratio of induced dipole moment to the intensity of the electric field. The induced dipole moment is proportional to polarizability and reactivity indication [43]. High values of polarizability facilitate the strong adsorption process of corrosion inhibitors onto the metal surface and hence, high inhibition efficiency. The polarizabilities were evaluated using equation (8) for the two inhibitors. As can be seen, the polarizabilities are in the order T2>T1, which correlates well with the corrosion inhibition efficiency observed.

Lipophilicity is important physicochemical property of an inhibitor, it plays a role in solubility, absorption, distribution. Lipophilicity tells about the compounds ability to dissolve into lipohilic (non-aqueous) solutions.

The most commonly used measure of lipophilicity is log *P*, this is the partition coefficient of a molecule between non-aqueous and aqueous phase. The partition coefficient is a measure of the difference in solubility of the compound in these two phases.

Hence the partition coefficient is measures of hydrophilic (water-loving) or hydrophobic (water-fearing) a chemical substance. Inhibitors which are hydrophobic (lipophilic) tends to have more Log *P* values and hydrophilic (lipophobic) inhibitors have less log *P*. If log *P* value is lower therefor inhibitor is more hydrophilic, Hence, it could be argued that inhibitor has the more tendency to absorb on the metal surface[49].

As can be seen from Table 1, it can be observed that the values of log *P* of T2 was lower than T1 The lower value of log *P* probably enhances the adsorption on the metal surface, so the corrosion inhibition efficiencies of T2 increases due to the enhancement of solubility in water .

Local reactivity was discussed to analysis active sites of inhibitor molecules, due to estimate the exact active atoms of inhibitor molecules.

The local indices such as natural atomic charge, distribution of frontier molecular orbital and Fukui functions are commonly used to analysis the behavior of the active sites of inhibitor molecules. Charges of atoms for the studied inhibitors in solution phase are listed in Table 2 and 3, which were calculated from the Hirshfeld population analysis (HPA)[50, 51].

It was found that the S and O atoms have the highest negative Charge in studied inhibitors, then these sites will preferably react as an electron donor. As seen in Table 2 and 3, negative charges on S and O atoms of

T2 are more than negative charges on S and O atoms of T1.

The total negative charge (TNC) is obtained by summing up the negative charges on atoms of the inhibitors [12, 52]. TNC of the two inhibitors is listed in Table 4. It is clear from Table 4 that T2 (-2.05) has the higher TNC value than T1 (-1.71).

Table 2. The calculated Fukui functions and charge for the selected atoms of the T1 inhibitor

T1	N	$N+1$	$N-1$	F^+	F^-
1 N	0.1009	0.0882	0.1257	0.0127	0.0247
2 C	0.1088	0.0998	0.1302	0.0090	0.0214
3 S	**-0.3791**	-0.4188	-0.1592	**0.0397**	**0.2198**
4 N	0.1021	0.0904	0.1533	0.0117	**0.0512**
6 N	0.1452	0.1144	0.2268	**0.0308**	**0.0815**
8 C	0.1209	0.0841	0.1533	0.0368	0.0323
9 S	**-0.3723**	-0.4767	0.0002	**0.1044**	**0.3725**
10 N	0.0894	0.0647	0.1204	0.0246	0.0310
12 C	0.1969	0.1463	0.2066	**0.0505**	0.0097
13 O	**-0.2786**	-0.3287	-0.2626	**0.0501**	0.0160
14 C	-0.0206	-0.0358	-0.0196	0.0152	0.0010
15 C	0.0265	-0.0063	0.0320	0.0328	0.0054
16 C	0.0238	-0.0107	0.0312	0.0345	0.0074
17 C	0.0263	0.0023	0.0319	0.0239	0.0056
19 C	0.0258	0.0014	0.0317	0.0243	0.0059
21 C	0.0376	-0.0047	0.0458	0.0424	0.0081
24 N	0.1542	0.1241	0.1729	0.0301	0.0187
27 C	0.1228	0.0873	0.1291	0.0355	0.0062
28 N	0.0910	0.0674	0.0968	0.0236	0.0057
29 S	**-0.3631**	-0.4657	-0.3024	**0.1026**	**0.0605**
30 C	0.1976	0.1495	0.1997	0.0481	0.0020
31 C	-0.0204	-0.0350	-0.0203	0.0145	0.0001
32 C	0.0240	-0.0096	0.0260	0.0336	0.0020
33 C	0.0272	-0.0037	0.0284	0.0309	0.0012
34 C	0.0259	0.0024	0.0276	0.0234	0.0017
36 C	0.0269	0.0037	0.0284	0.0232	0.0014
38 C	0.0377	-0.0032	0.0401	0.0410	0.0022
41 O	**-0.2790**	-0.3278	-0.2755	0.0487	0.0034

Another parameters that were considered are the total number of charge centers (negative and positive). The negative and positive charge centers (NCC and PCC) show donating and accepting electrons in inhibitor. Higher total number of charge centers of T2 (Table 4) indicated that chemical bond between T2 -Fe surface stronger than T1 -Fe surface.

Table 3. The calculated Fukui Functions and Charge for the selected atoms of the T2 inhibitor

T2	*N*	*N+1*	*N-1*	*F⁺*	*F⁻*
1 N	0.1017	0.0880	0.1309	0.0136	0.0292
2 C	0.1091	0.0975	0.1296	0.0115	0.0205
3 S	**-0.3882**	-0.4334	-0.1789	**0.0451**	**0.2093**
4 N	0.1028	0.0895	0.1411	0.0132	0.0383
6 N	0.1480	0.1159	0.2072	0.0321	**0.0591**
8 C	0.1208	0.0807	0.1453	0.0401	0.0244
9 S	**-0.3792**	-0.4891	-0.1009	**0.1099**	**0.2782**
10 N	0.0852	0.0608	0.1097	0.0243	0.0245
12 C	0.1909	0.1435	0.1976	0.0474	0.0066
13 O	**-0.2861**	-0.3332	-0.2752	0.0471	0.0108
14 C	-0.0365	-0.0478	-0.0330	0.0112	0.0034
15 C	0.0323	0.0014	0.0385	0.0308	0.0062
16 C	0.0253	-0.0044	0.0324	0.0297	0.0071
17 C	-0.0007	-0.0184	0.0062	0.0183	0.0063
19 C	0.0025	-0.0171	0.0101	0.0197	0.0076
21 C	0.0922	0.0714	0.0976	0.0207	0.0053
24 O	**-0.1331**	-0.1445	-0.1280	0.0113	0.0050
25 C	0.1691	0.1556	0.1743	0.0135	0.0052
29 N	0.1509	0.1183	0.1871	0.0326	0.0362
32 C	0.1215	0.0808	0.1358	0.0407	0.0142
33 N	0.0858	0.0615	0.0994	0.0243	0.0135
34 S	**-0.3757**	-0.4875	-0.2232	**0.1117**	**0.1525**
35 C	0.1915	0.1441	0.1954	0.0474	0.0039
36 C	-0.0367	-0.0480	-0.0352	0.0112	0.0015
37 C	0.0289	-0.0048	0.0334	0.0337	0.0044
38 C	0.0292	0.0022	0.0323	0.0270	0.0030
39 C	-0.0001	-0.0184	0.0037	0.0183	0.0038
41 C	0.0032	-0.0165	0.0070	0.0197	0.0038
43 C	0.0922	0.0715	0.0952	0.0207	0.0029
46 O	**-0.2855**	-0.3324	-0.2791	0.0469	0.0063
47 O	**-0.1332**	-0.1445	-0.1305	0.0113	0.0026
48 C	0.1692	0.1557	0.1721	0.0135	0.0028

Table 4. The interaction energy obtained from MD simulation for adsorption of inhibitors on Fe (110) surface. The total negative charge (TNC), the total number of the negative charge centers (NCC) and the positive charge centers (PCC) of the studied inhibitors in aqueous phase

system	$E_{interaction}$ (kcal/mol)	TNC(ev)	NCC	PCC
T1	-1906.1988	-1.713	7	21
T2	-1996.4465	-2.054	11	21

T1 (a)   **T1(b)**

T2(a)   **T2 (b)**
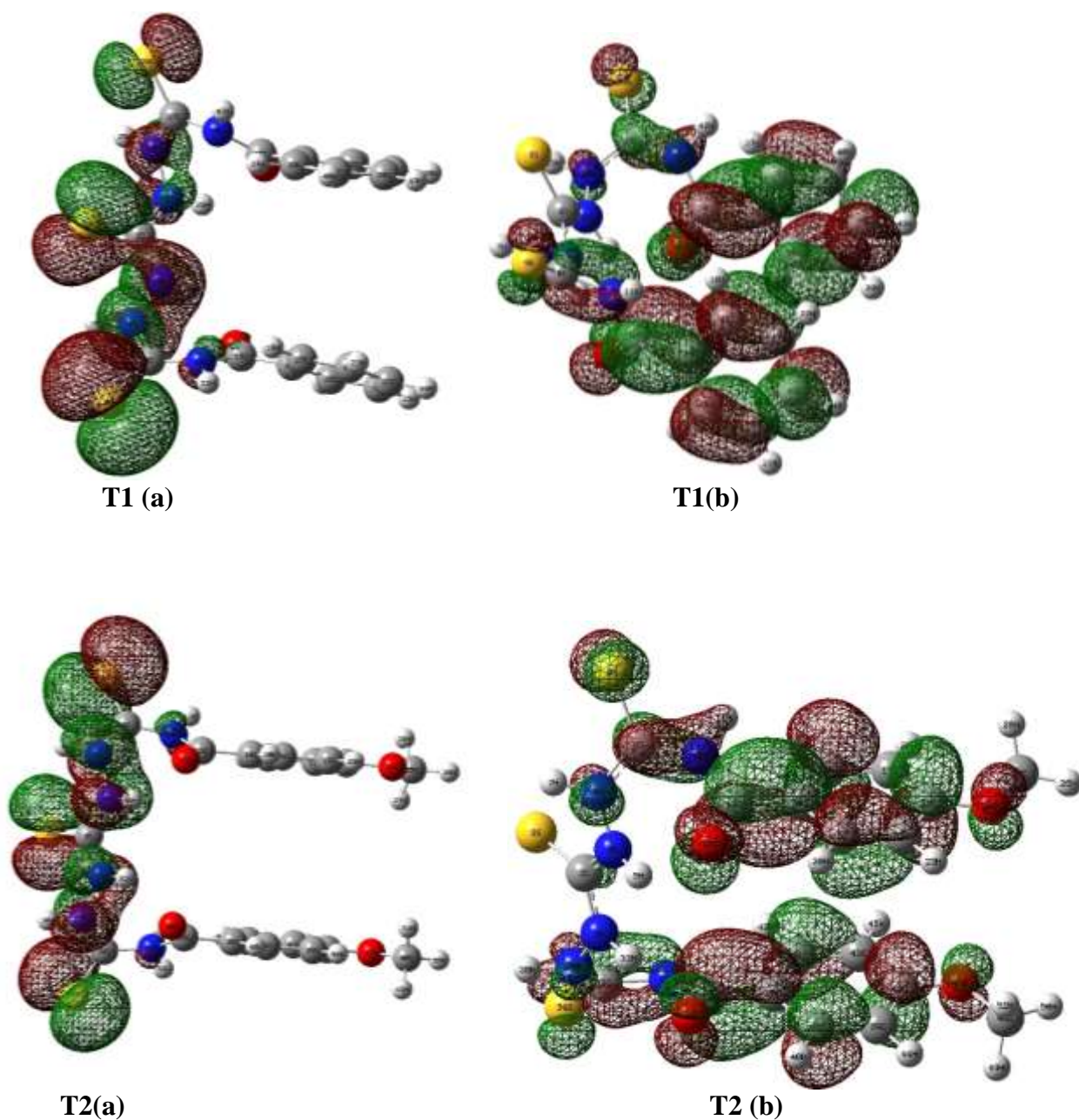
Figure 2. The frontier molecule orbital density distribution of the investigated inhibitors: (a) HOMO, (b) LUMO

The electron density distribution of the HOMO and LUMO orbitals are shown in Figure. 2.

The HOMO electron density distribution indicates the reactive sites of the inhibitors that have a tendency to donate electrons to electrophilic species whereas the LUMO electron density distribution predicts the regions of the molecule with high tendency to accept electrons from nucleophilic species. In each two inhibitors, the HOMO is strongly localized on S and N atoms while the LUMO is localized on the entire molecule with the exception of S3, C2, N4, N1, C25 and C48 atoms.

Tables 2 and 3 show condensed Fukui indices, the atoms of molecule which accepting electrons have more $F^+(r)$ (the index for nucleophilic attack); when the atoms of molecule which donating electrons have more $F^-(r)$ (the index for electrophilic attack for an inhibitor molecule). It is evident that the preferred site for nucleophilic attack and electrophilic attack for the two inhibitors are S atoms, which indicated that these atoms will be the most probable nucleophilic and electrophilic reactive sites during the absorption.

The calculated Fukui functions are in good agreement with the results of the electron density distribution of the frontier orbitals.

In spite of advancements in quantum chemical techniques, due to computationally expensive for systems involving a large number of molecules, Molecular dynamics (MD) simulation usually only applied to these systems. Many corrosion inhibition studies nowadays contain the use of molecular dynamics simulation as an important tool in understanding the interaction between adsorbate-metal surfaces [53-56]. It has been reported that the more negative the adsorption energies, the stronger the adsorbate-metal interaction [57].
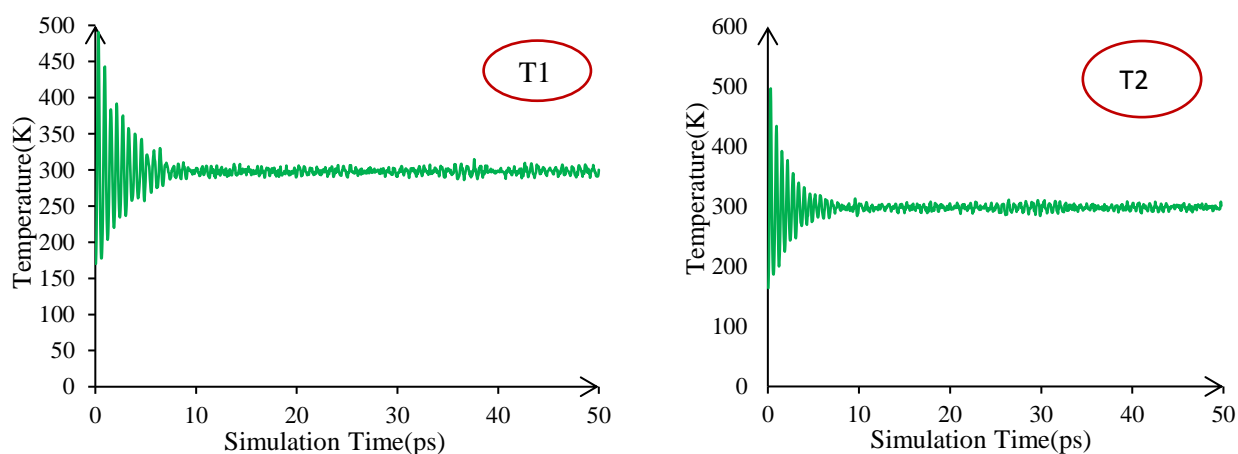

Figure 3. Temperature equilibrium curve obtained from molecular dynamics simulation for T2 and T1
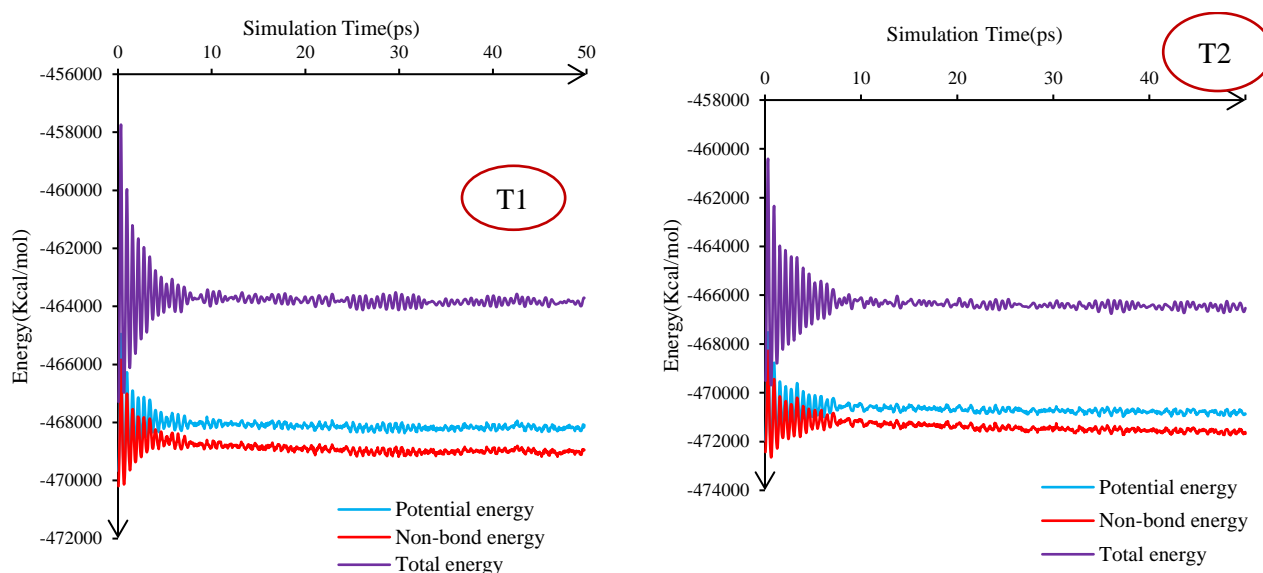
Figure 4. Energy fluctuant curve obtained from molecular dynamics simulation for T1 and T2

In this study, two selected inhibitors have been placed on the Fe (1 1 0) surface to find out their suitable configuration. To examine the equilibrium state of systems, diagrams of temperature and energy obtained *via* MD simulations were analyzed.
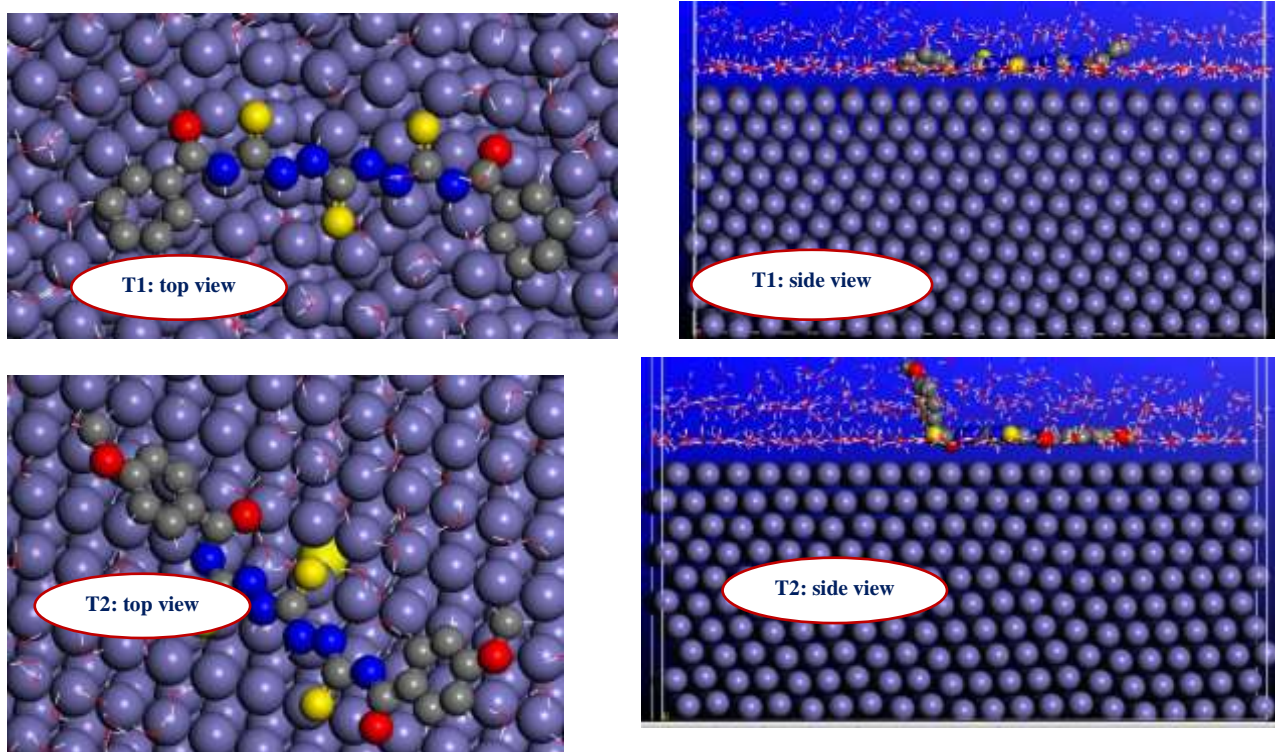

Figure 5. Equilibrium adsorption configurations of inhibitors T1 and T2 on Fe (1 1 0) surface obtained by molecular dynamics simulations

The Figures 3 and 4 show temperature and energy fluctuation curve as a function of time. fluctuations of The temperature are in a range of (298± 5) K and the fluctuations of energy are less than 0.5%, indicating that the system has reached an equilibrium state[58]. The system equilibrium state and the best adsorption configurations of the surface-adsorbed inhibitor are depicted in Figure 5.

As can be seen from Figure 5, inhibitor molecules have a parallel orientation with respect to the iron surface. The interaction between the inhibitors and the Fe surface is in a parallel orientation from the surface.

The potential and total energies of a system are simple measure of system stability. Analysis of energy curve revealed that both the T2 and T1 systems in the simulation were well equilibrated and remained stable throughout the simulation of 50 ps (Figures 3 and 4). However, potential energy plots show that the potential energy for T2 system remains more negative (Approximately -470853.3315 kcal mol^{-1}) as compared to T1 system (approximately -468088.8472627 kcal mol^{-1}) (Figure 4). This result indicates that the T2 system, on an average, was more stable than the T1 system.

Similarly, the total energy plots also indicate that the total energy for T2 remains more negative (approximately -466527.1571 kcal mol^{-1}) as compared to T1 (Approximately -463711.0532 kcal mol^{-1}), confirming the structural stability of T2 system as compared to T1 system (Figure 4). Interaction energy, which results from the binding of inhibitor to iron surface, was calculated to measure the stability of inhibitor-Fe(110) complexes.

The values of the interaction energies of the two inhibitors on Fe(110) surface are listed in Table 4. It is evident from Table 4 that T2 has the higher negative interaction energy as compared to the T1 case system. Therefore, the adsorption of T2 on the iron surface in aqueous solution is easier than T1. Values of negative interaction energy for two inhibitors suggests that the adsorption on mild steel surface is spontaneous.

Radial Distribution Functions (RDFs (g(r))) based on trajectories generated by molecular dynamics simulation method are used to distinguish the type of molecule–surface interaction. As a basic rule, the peak in the g(r) curve within 3.5 Å is caused by Chemisorption, and that outside 3.5 Å is caused by physisorption [58].
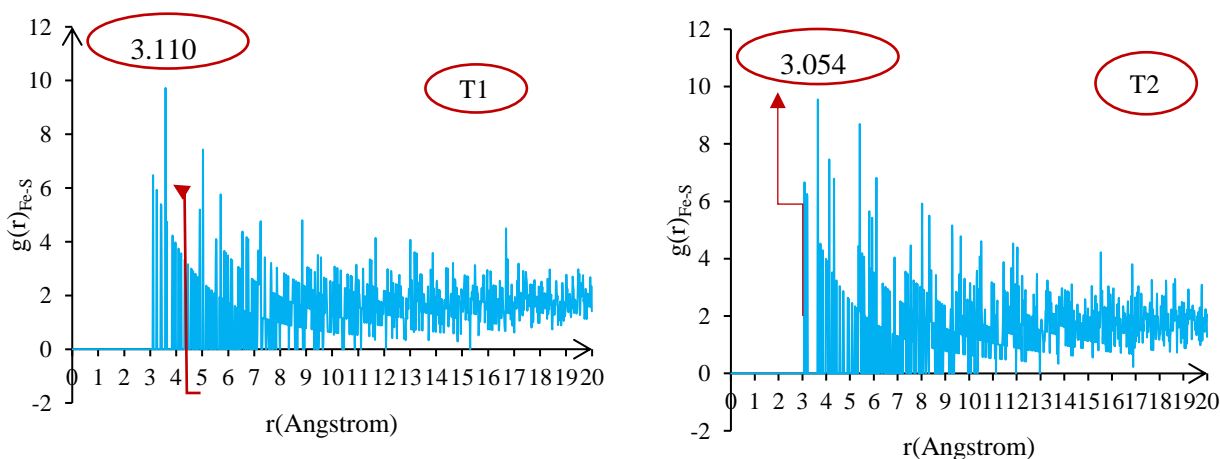

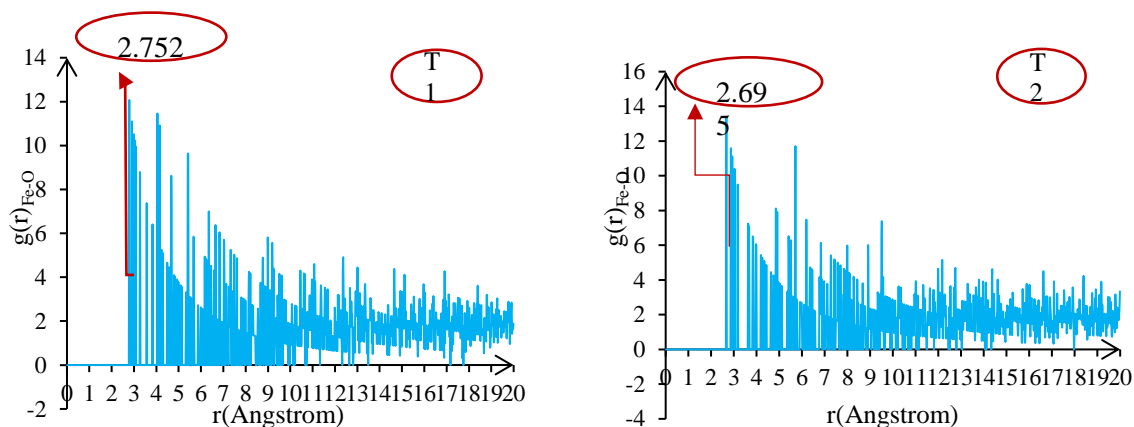**Figure 6.** RDF curves of S–Fe after MD simulations

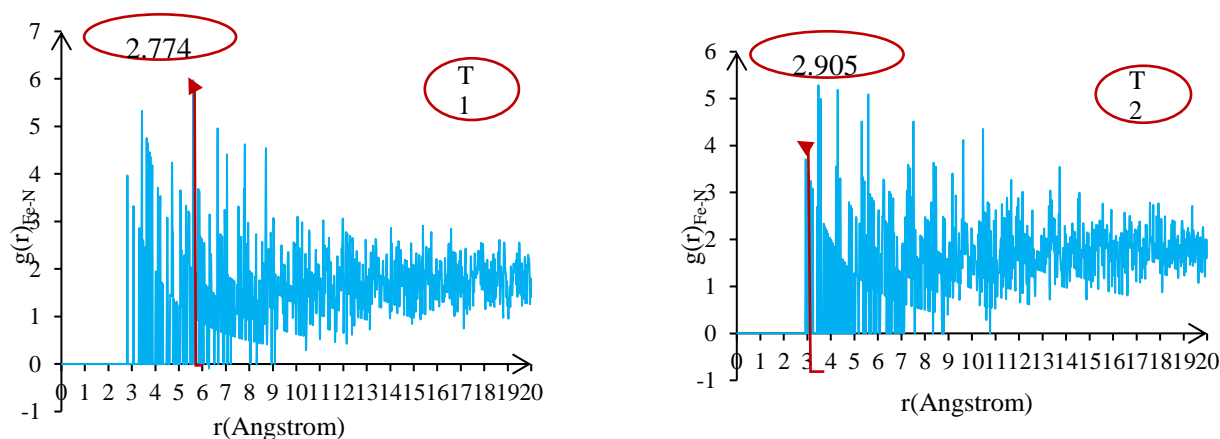**Figure 7.** RDF curves of O–Fe after MD simulations

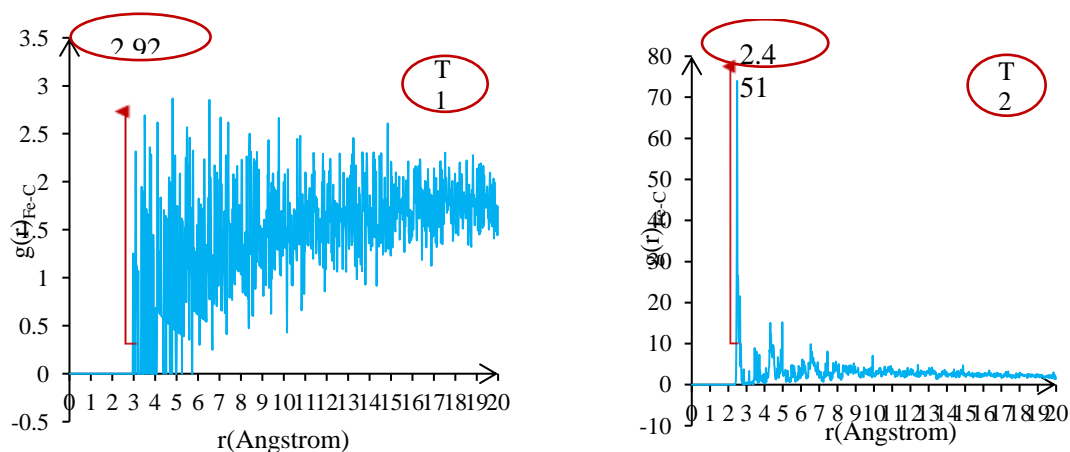**Figure 8.** RDF curves of N–Fe after MD simulations

Figure 9. RDF curves of C–Fe after MD simulations

As shown in Figures 6, 7, 8 and 9 (The first peak on RDF represents the most probable distance between inhibitors atoms and Fe atoms), peak value of inhibitors atoms (S, N, O and C atoms) -Fe RDF are in a less range from 3.5 Å, which indicated that chemical bonds have formed between these two inhibitors and iron atoms.

T2 has the strongest interaction with the metal surface. These results are also supported by the comparison of the bond distances (Figures 6, 7, 8 and 9) that show that atoms of T2(S, O and C atoms) have the shorter bond distance (therefore stronger interactions between T2 and the Fe atom) than T1. The RDF plot obtained from the interaction between N of T2 and Fe showed a peak at 2.905, indicating the presence of weaker interactions between N atom of T2 and Fe than N atom of T1 and Fe. Both results (the interaction energy and the bond distances), confirm that T2 has a stronger adsorption on the metal surface.

Conclusion

Inhibition efficiencies of two thiocarbohydrazide derivatives (*N,N'*-[2,2'-thiocarbonyl bis(hydrazine-2,1-diyl) bis (thioxomethylene)] dibenzamide (T1) and *N,N'*-[2,2'-thiocarbonylbis(hydrazine-2,1- diyl) bis (thioxomethylene)] bis (4-methoxybenzamide) (T2) has been studied on corrosion of carbon steel using quantum chemical parameters and Molecular dynamics (MD) simulation method in aqueous phase. Quantum chemical parameters electrophilicity (ω), Electronegativity (χ), polarizability (α), dipole moment (μ), E_{HOMO} (the energy of the highest occupied molecular orbital), the total amount of electronic charge transferred (ΔN), Lipophilicity, total negative charges on the whole of the molecule (TNC), molecular volume (MV), surface area and Fukui index are in consistent with the experimental inhibition efficiency and confirm the reliability of quantum chemical method. Molecular dynamics simulation results showed that T2 inhibitor has the higher negative interaction energy as compared to the T1 inhibitor.

Radial Distribution Functions (RDFs) peak of inhibitors atoms (S, N, O and C atoms) - Fe (110) are in a less range from 3.5 Å, which indicated that inhibitors is chemisorbed on surface. Also the RDF plot obtained from the interaction between atoms of T2 and Fe (110) surface indicating stronger interactions T2 with Fe (110).

Results of DFT and MD simulations calculations confirm that T2 has more inhibition efficiency than T1, which is in good agreement with the experimentally inhibition efficiency data reported.

References
[1] T.P. Swiler, R.E. Loehman, *Acta Materialia*, **2000**, *48*, 4419-4424.
[2] A. Kornherr, S.A. French, A.A. Sokol, C.R.A. Catlow, S. Hansal, W.E.G. Hansal, J.O. Besenhard, H. Kronberger, G.E. Nauer, G. Zifferer, *Chemical Physics Letters*, **2004**, *393*, 107-111.
[3] A. Kornherr, S. Hansal, W.E.G. Hansal, J.O. Besenhard, H. Kronberger, G.E. Nauer,G. Zifferer, *The Journal of Chemical Physics*, **2003**, *119*, 9719-9728.
[4] K.F. Khaled, A.M. El-Sherik, *International Journal of Electrochemical Scince*, **2013**, *8*, 10022-10043.
[5] G. Gece, *Corrosion Science*, **2008**, *50*, 2981-2992.
[6] I.B. Obot,N.O. Obi-Egbedi, *Corrosion Science*, **2010**, *52*, 657-660.
[7] A.Y. Musa, A.A.H. Kadhum, A.B. Mohamad, M.S. Takriff, *Corrosion Science*, **2010**, *52*, 3331-3340.
[8] H. Ju, Z.-P. Kai,Y. Li, *Corrosion Science*, **2008**, *50*, 865-871.

[9] E.E. Ebenso, D.A. Isabirye, N.O. Eddy, *Int J Mol Sci*, **2010**, *11*, 2473-2498.

[10] T. Arslan, F. Kandemirli, E.E. Ebenso, I. Love, H. Alemu, *Corrosion Science*, **2009**, *51*, 35-47.

[11] J.M. Roque, T. Pandiyan, J. Cruz, E. García-Ochoa, *Corrosion Science*, **2008**, *50*, 614-624.

[12] M.S. Masoud, M.K. Awad, M.A. Shaker, M.M.T. El-Tahawy, *Corrosion Science*, **2010**, *52*, 2387-2396.

[13] A. Popova, M. Christov, A. Zwetanova, *Corrosion Science*, **2007**, *49*, 2131-2143.

[14] M.K. Awad, R.M. Issa,F.M. Atlam, *Materials and Corrosion*, **2009**, *60*, 813-819.

[15] R.M. Issa, M.K. Awad, F.M. Atlam, *Materials and Corrosion*, **2010**, *61*, 709-714.

[16] G. Gece, *Materials and Corrosion*, **2013**, *64*, 940-944.

[17] M. Dehdab, Z. Yavari, M. Darijani, A. Bargahi, *Desalination*, **2016**, *400*, 7-17.

[18] M. Dehdab, M. Shahraki,S.M. Habibi-Khorassani, *Amino Acids*, **2016**, 48, 291-306.

[19] N. Esmaeili, J. Neshati, I. Yavari, *Journal of Industrial and Engineering Chemistry*, **2015**, *22*, 159-163.

[20] A.D. Becke, *Phys Rev A*, **1988**, *38*, 3098-3100.

[21] A.D. Becke, *The Journal of Chemical Physics*, **1993**, *98*, 5648-5652.

[22] C. Lee, W. Yang, R.G. Parr, *Physical Review B*, **1988**, *37*, 785-789.

[23] M.J.T. Frisch, G. W. Schlegel, H. B. Scuseria, G.E. Robb, M.A. Cheeseman, J.R. Montgomery, Jr., J.A. Vreven, T. Kudin, K.N. Burant, J.C. Millam, J.M. Iyengar, S.S. Tomasi, J. Barone, V. Mennucci, B. Cossi, M. Scalmani, G. Rega, N. Petersson, G.A. Nakatsuji, H. Hada, M. Ehara, M. Toyota, K. Fukuda, R. Hasegawa, J. Ishida, M. Nakajima, T. Honda, Y. Kitao, O. Nakai, H. Klene, M. Li, X. Knox, J.E. Hratchian, H.P. Cross, J.B. Bakken, V. Adamo, C. Jaramillo, J. Gomperts, R. Stratmann, R.E. Yazyev, O. Austin, A.J. Cammi, R. Pomelli, C. Ochterski, J.W. Ayala, P.Y. Morokuma, K. Voth, G.A. Salvador, P. Dannenberg, J.J. Zakrzewski, V.G. Dapprich, S. Daniels, A.D. Strain, M.C. Farkas, O. Malick, D.K. Rabuck, A.D. Raghavachari, K. Foresman, J.B. Ortiz, J.V. Cui, Q. Baboul, A.G. Clifford, S. Cioslowski, J. Stefanov, B.B. Liu, G. Liashenko, A. Piskorz, P. Komaromi, I. Martin, R.L. Fox, D.J. Keith, T. Al-Laham, M.A. Peng, C.Y. Nanayakkara, A. Challacombe, M. Gill, P.M.W. Johnson, B. Chen, W. Wong, M.W. Gonzalez, C. Pople, J.A., Gaussian 03, Revision C.02(Gaussian, Inc., Wallingford CT), **2004**.

[24] S. Miertuš, E. Scrocco,J. Tomasi, *Chemical Physics*, **1981**, *55*, 117-129.

[25] R.G. Parr,W. Yang, Density Functional Theory of Atoms and Molecules, (Oxford University Press, Oxford), **1989**.

[26] R.G. Parr,R.G. Pearson, *Journal of the American Chemical Society*, **1983**, *105*, 7512-7516.

[27] T. Koopmans, *Physica*, **1934**, *1*, 104-113.

[28] C.-G. Zhan, J.A. Nichols, D.A. Dixon, *The Journal of Physical Chemistry A*, **2003**, *107*, 4184-4195.

[29] R.G. Parr, L.V. Szentpály,S. Liu, *Journal of the American Chemical Society*, **1999**, *121*, 1922-1924.

[30] A.T. Maynard, M. Huang, W.G. Rice, D.G. Covell, *Proc Natl Acad Sci U S A*, **1998**, *95*, 11578-11583.

[31] R.G. Pearson, *Inorganic Chemistry*, **1988**, *27*, 734-740.

[32] K.F. Khaled, *Electrochimica Acta*, **2010**, *55*, 6523-6532.

[33] N. Kovačević,A. Kokalj, *The Journal of Physical Chemistry C*, **2011**, *115*, 24189-24197.

[34] M. Yadav, D. Behera, S. Kumar, R.R. Sinha, *Industrial & Engineering Chemistry Research*, **2013**, *52*, 6318-6328.

[35] A. Kokalj, *Electrochimica Acta*, **2010**, *56*, 745-755.

[36] I. Obot, D. Macdonald,Z. Gasem, *Corrosion Science*, **2015**, *99*, 1-30.

[37] A. Kokalj, *Chemical Physics*, **2012**, *393*, 1-12.

[38] J. Zevallos, A. Toro-Labbé, *Journal of the Chilean Chemical Society*, **2003**, *48*, 39-47.

[39] T.K. Ghanty, S.K. Ghosh, *The Journal of Physical Chemistry*, **1993**, *97*, 4951-4953.

[40] M. Studio, in 6.1Manual, Accelrys, Inc., San Diego, CA. **2007**.

[41] J.-M. Zhang, D.-D. Wang, K.-W. Xu, *Applied Surface Science*, **2006**, *252*, 8217-8222.

[42] K. Fukui, *Angewandte Chemie International Edition in English*, **1982**, *21*, 801-809.

[43] E.E. Ebenso, T. Arslan, F. Kandemirli, N. Caner, I. Love, *International Journal of Quantum Chemistry*, **2010**, *110*, 1003-1018.

[44] R.G. Pearson, *Journal of Chemical Education*, **1968**, *45*, 581-584.

[45] R.G. Pearson, *Journal of Chemical Education*, **1968**, *45*, 643-648.

[46] Mahendra Yadav, Sushil Kumar, Indra Bahadur, D. Ramjugernath, *International Journal of Electrochemical Scince*, **2014**, *9*, 6529-6550.

[47] I. Lukovits, E. Kalman,F. Zucchi, *Corrosion*, **2001**, *57*, 3-8.

[48] X. Li, S. Deng, H. Fu,T. Li, *Electrochimica Acta*, **2009**, *54*, 4089-4098.

[49] A.M. Al-Sabagh, N.M. Nasser, A.A. Farag, M.A. Migahed, A.M. Eissa, T. Mahmoud, *Egyptian Journal of Petroleum*, **2013**, *22*, 101-116.

[50] F.L. Hirshfeld, *Theoretica chimica acta*, **1977**, *44*, 129-138.

[51] F. De Proft, C. Van Alsenoy, A. Peeters, W. Langenaeker, P. Geerlings, *Journal of Computational Chemistry*, **2002**, *23*, 1198-1209.

[52] S.E. Nataraja, T.V. Venkatesha, H.C. Tandon, *Corrosion Science*, **2012**, *60*, 214-223.

[53] Y. Tang, X. Yang, W. Yang, Y. Chen, R. Wan, *Corrosion Science*, **2010**, *52*, 242-249.

[54] S. Xia, M. Qiu, L. Yu, F. Liu,H. Zhao, *Corrosion Science*, **2008**, *50*, 2021-2029.

[55] Y. Tang, L. Yao, C. Kong, W. Yang,Y. Chen, *Corrosion Science*, **2011**, *53*, 2046-2049.

[56] L. Feng, H. Yang, F. Wang, *Electrochimica Acta*, **2011**, *58*, 427-436.

[57] K.F. Khaled, *Journal of Applied Electrochemistry*, **2011**, *41*, 423-433.

[58] J. Zeng, J. Zhang,X. Gong, *Computational and Theoretical Chemistry*, **2011**, *963*, 110-114.